Enhancing Average Secrecy Rates in Downlink NOMA with Dependent Channel Coefficients and Optimal Power Coefficients[*]

Research Article

Faramarz Aajami Khales[1]   Ghosheh Abed Hodtani[2]

Abstract: Wireless communication systems demand efficient solutions, and non-orthogonal multiple access (NOMA) has emerged as a promising approach. The present investigation compares NOMA against orthogonal multiple access (OMA) methods, specifically focusing on TDMA. Through an analysis of the performance metrics, specific optimal power coefficients were derived, ensuring superior performance of NOMA schemes. It is important to note that these optimal power coefficients are dependent on the channel coefficients, meaning they will vary as the channel conditions of the users change. Using copula functions, we modeled the dependence between the channel coefficients and successfully obtained the dependences among the fading coefficients. Utilizing specific optimal power coefficients, calculations for the average secrecy rates of NOMA were conducted, considering the modeled dependencies. The analysis of mathematical and numerical results in this study reveals a significant performance improvement in the average secrecy rates of Downlink NOMA when considering dependent channel coefficients and optimal specific coefficients, as compared to independent NOMA.

Keywords: Wireless communication systems, Non-orthogonal multiple access (NOMA), Optimal power coefficients, Copula functions, Average secrecy rate.

1. Introduction

Efficient solutions in wireless communication systems are essential in order to effectively respond to the growing demand for connectivity. NOMA has emerged as a promising wireless communication scheme, enabling multiple users to efficiently share channel resources. It offers a solution for simultaneous user deployment, enhancing resource utilization in wireless networks. This study presents a thorough comparison of NOMA and orthogonal multiple access (OMA) schemes, with a specific focus on time division multiple access (TDMA). The main goal of this research is to analyze performance metrics and determine optimal power coefficients that guarantee superior performance in NOMA systems.

An investigation was carried out on the NOMA scheme, with a particular emphasis on evaluating the influence of optimal specific coefficients on the average secure rate of users. The influence of the correlation among the channel coefficients and its impact on secure rate performance was studied. For modeling the interrelation among channel fading coefficients, copula functions were employed, facilitating accurate expression and analysis of the interdependencies. Through the calculation of optimal specific coefficients and the application of copula functions, insights were obtained concerning the importance of coefficient dependence and its effects on enhancing secure

rate performance within NOMA systems.

In [1], a review of various NOMA schemes for 5G cellular networks offers valuable insights into their performance suitability and potential for future wireless systems. In [2], a comprehensive analysis and comparison of NOMA techniques is conducted, taking into account various performance measures and exploring their implications for next-generation networks. In [3-5], a comparison between NOMA and OMA schemes examines their performance and investigates the potential advantages of NOMA over OMA in wireless communication systems. NOMA is a promising technology that outperforms OMA (Orthogonal Multiple Access) and holds significant potential for integration into IoT (Internet of Things) systems [6]. The main idea of NOMA is to employ multiple different users on the same channel resources but with different power levels, which can improve system capacity.

Investigating physical layer security (PLS) in NOMA in order to increase security in wireless communication system is considered according to NOMA features. PLS in NOMA focuses on secure communication between legitimate users while thwarting eavesdropping. In various articles to examine the security of the physical layer in NOMA on various topics such as user pairing, optimizing power allocation, employing artificial noise to confuse eavesdroppers, and utilizing beamforming and precoding techniques.

In [7], a survey offers an overview of physical layer security techniques in NOMA systems, while [8] explores challenges and opportunities for achieving physical layer security in NOMA networks. [9] investigates physical layer security methods tailored for NOMA in 5G networks, and [10] provides a review of physical layer security techniques in the context of NOMA. Additionally, [11] proposes solutions and addresses challenges related to physical layer security in NOMA systems.

In the referenced article [12], the researchers studied how the correlation between fading coefficients influences the wiretap channel's behavior. In the present study, the focus was shifted to understanding how this dependence impacts the Downlink NOMA. The approach of evaluating secrecy rates under both the assumptions of independence and dependence among fading coefficients contributes significantly to advancing the understanding of NOMA downlink systems. It not only provides a comprehensive perspective but also allows for a more nuanced interpretation of how secrecy rates vary in different scenarios. Incorporating the dependence between fading coefficients is a crucial step towards improving the accuracy of average secrecy rate calculations in NOMA systems. While it introduces complexity, it also provides a more realistic

representation of channel conditions, which is essential for making informed decisions in the design and operation of secure and efficient wireless communication systems. Future research should continue to explore the nuances of fading coefficient dependence and develop efficient techniques for its inclusion in NOMA analysis.

Our work. in this study, the contributions are summarized as follows:

1. Comparative Evaluation: A thorough comparison is conducted between NOMA and OMA schemes, with a specific focus on TDMA, in order to quantify the advantages of NOMA in wireless communication systems.
2. Optimal Power Coefficients: Specific optimal power coefficients are derived through a comprehensive analysis of performance metrics, ensuring the enhanced performance of NOMA schemes.
3. Modeling Channel Dependencies: By employing copula functions, the dependence among channel coefficients is modeled, enabling the accurate capture and understanding of the correlation among fading coefficients.
4. Secrecy Rate Analysis: The average secrecy rates of NOMA are calculated and analyzed by incorporating the modeled dependencies and optimal power coefficients. This analysis showcases the improvements achieved by considering dependent channel coefficients and optimal coefficients.
5. Performance Enhancement: The mathematical and numerical analysis demonstrates a notable enhancement in the average secrecy rates of Downlink NOMA. This indicates the effectiveness of the proposed approach in real-world scenarios with varying channel conditions and interdependencies.

2. Introduction to the Utilized System Mode
2.1. System model of Downlink NOMA
The investigated system, as shown in Fig. 1, includes a base station (BS) on the transmitter side, while on the receiver side it includes two legitimate receivers and one eavesdropping receiver. All transmitters and receivers of this system are equipped with an antenna. Using the superposition coding (SC) technique at the BS, a superimposed signal (x) is generated that contains messages intended for legitimate users. This combined signal is then transmitted to all receivers via wireless channels.

$$x = \sqrt{\alpha_m P} x_m + \sqrt{\alpha_n P} x_n \qquad (1)$$

where x_m and x_n are messages of strong and weak users, respectively. α_m and α_n represent the power coefficients assigned to send the message of the m-th and n-th user, respectively and P is the total transmitted power. The transmitted messages have a unit power, denoted as $\mathbb{E}\{|x_i|^2\} = 1 \ (i = m, n)$, where $\mathbb{E}\{\}$ represents the expectation operator. Additionally, the total allocation of transmission power coefficients satisfies the condition $(\alpha_m + \alpha_n = 1)$.

To ensure fairness in user rates within NOMA, the user with a weaker channel state is allocated a higher transmission power i.e. $(\alpha_n \geq \alpha_m)$. This allocation strategy aims to compensate for the weaker channel condition and provide equitable opportunities for users to achieve comparable rates in the NOMA system.

The received signal at user i can be expressed as follows:

$$y_i = h_i x + n_i \qquad i = m, n, e \qquad (2)$$

where h_i represents the channel gain between the transmitter and user i, x is the message sent from the BS, and n_i is an independent and identically distributed (i.i.d.) circularly symmetric complex Gaussian random variable with zero mean and variance N_i. In this case, for simplicity, it is assumed that the noise variances at all users are equal, denoted as $\sigma_m^2 = \sigma_n^2 = \sigma_e^2 = N$.
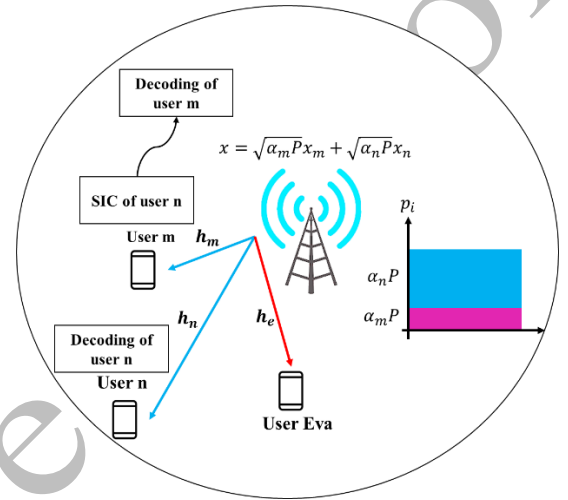

Figure 1. illustration of a Downlink NOMA system with two users (strong and weak) and an eavesdropper

In the downlink NOMA scheme, the successive interference cancellation (SIC) technique is utilized to decode the messages of individual users. The receivers follow a specific order where they first decode the message of the weaker user, treating the message of the stronger user as combined interference, including the background noise. Afterward, the revealed message of the weaker user is subtracted from the overall received signal at the receivers. This iterative process allows the stronger user to decode their message without the interference caused by the weaker user's message. By sequentially canceling interference, NOMA efficiently utilizes resources and enables multiple users to achieve reliable communication in the downlink transmission. By utilizing the SC technique at the BS and employing the SIC technique at the receivers, the rates of each user in downlink NOMA can be expressed as follows:

$$R_m^{NOMA} = \log(1 + \frac{\alpha_m P |h_m|^2}{N}) \qquad (3)$$

$$R_n^{NOMA} = \log(1 + \frac{\alpha_n P |h_n|^2}{\alpha_m P |h_n|^2 + N}) \qquad (4)$$

2.2. Optimum power coefficients in Downlink NOMA
The NOMA scheme offers distinct advantages over the OMA scheme. The sharing of the same time frequency resources by several different users in NOMA can be

mentioned, which improves the spectral efficiency and increases the system capacity. By allocating different power levels to users, NOMA enables simultaneous access to the same resources and increases spectral efficiency. In contrast, OMA allocates separate time-frequency resources to each user, which results in lower spectral efficiency and reduced capacity. By comparing the rates obtained in NOMA with the OMA rates, a range of power coefficients is obtained that ensures the superiority of the NOMA rates over the corresponding orthogonal rates for both strong and weak users. This range of power coefficients signifies that NOMA can achieve higher rates compared to OMA for all users, regardless of their channel conditions. The findings highlight the advantages of NOMA in terms of improved spectral efficiency and enhanced capacity, making it a promising choice for future wireless communication systems.

Hence, through the comparison of NOMA rates and OMA rates, the relationships can be expressed as follows:

$$R_m^{NOMA} \geq R_m^{OMA} \rightarrow log_2(1 + \alpha_m \lambda_m) \geq \frac{1}{2} log_2(1 + \lambda_m) \quad (5)$$

$$R_n^{NOMA} \geq R_n^{OMA} \rightarrow log_2(1 + \frac{\alpha_n \lambda_n}{1 + \alpha_m \lambda_n}) \geq \frac{1}{2} log_2(1 + \lambda_n) \quad (6)$$

where the value of λ_i is equal to $\lambda_i = \frac{P|h_i|^2}{N}$ for $(i = m, n)$. Through simplification of (5), we arrive at the expression presented in (7) as follows:

$$a_m \geq \frac{1}{\sqrt{1 + \lambda_m} + 1} \quad (7)$$

Similarly, by simplifying (6), the range obtained for power factor α_m is expressed as follows:

$$a_m \leq \frac{1}{\sqrt{1 + \lambda_n} + 1} \quad (8)$$

To ensure the superiority of NOMA rates over OMA rates, the power factor α_m should fall within a specific range, as indicated by the relationship between (7) and (8). By selecting an appropriate value for the power factor, the advantages of NOMA in terms of higher rates and improved performance can be effectively realized, surpassing the corresponding rates achieved in orthogonal multiple access. Consequently, the (7) and (8) can be deduced from the given equation:

$$0 < \frac{1}{\sqrt{1 + \lambda_m} + 1} \leq a_m \leq \frac{1}{\sqrt{1 + \lambda_n} + 1} < 0.5 \quad (9)$$

To achieve the maximum sum of rates in a NOMA system, it is necessary to select an optimal power factor. This power factor strikes a balance between the superiority of NOMA rates compared to OMA rates and the overall rate maximization. The expression for the optimal power factor can be defined as follows:

$$\alpha_m^* = \frac{1}{\sqrt{1 + \lambda_n} + 1} \quad (10)$$

2.3. Joint probability density function based on copula functions

The copula function is a mathematical concept that is used in the field of statistics and probability theory to describe the structure of dependence between random variables. It provides a method for modeling the joint distribution of multiple variables independently of their marginal distributions. The copula function effectively captures the correlation or dependence between variables by transforming their marginal distributions into uniform distributions. Using the copula, it becomes possible to study and model complex dependencies that may not be adequately represented by simple correlation measures. Copula functions have various applications, such as being used in the fields of finance, risk management, and multivariate analysis, where understanding and modeling the dependence structure between variables is essential for accurate analysis and decision making [13-14].

The scalar theorem [15] provides a means to transform random variables into uniform distributions and is often used as a preliminary step in applying copula functions. The joint probability density function (PDF) for a multivariate distribution can be expressed using copula functions as follows:

$$f(\lambda_m, \lambda_n) = f(\lambda_m)f(\lambda_n)c(F(\lambda_m), F(\lambda_n)) \quad (11)$$

where $c(.)$ is the copula density function, $F(\lambda_i)$ is the marginal cumulative distribution function of variable λ_i ($i = m, n, e$), and $f(\lambda_i)$ is the marginal probability density function of variable x_i. Within this study, the Farlie-Gumbel-Morgenstern (FGM) copula is employed to empirically assess the performance criteria of the proposed system. The FGM copula is selected for its simplicity in calculating joint probability density functions (PDFs) [13], making it a suitable choice for our analysis. Moreover, FGM copulas allow for the consideration of both negative and positive correlations, as well as independence scenarios. By employing the FGM copula, the system's performance can be effectively assessed, allowing for an investigation of various correlation scenarios. This study employs the FGM copula to empirically analyze the performance metrics of the proposed system. The selection of the FGM copula stems from its computational simplicity in calculating joint probability density functions (PDFs) [13], rendering it an apt choice for the analysis. Furthermore, FGM copulas permit the examination of both negative and positive correlations, along with scenarios of independence. By employing the FGM copula, the evaluation of the system's performance is carried out effectively, facilitating the exploration of diverse correlation scenarios. The relationship of this copula is expressed as follows:

$$C(u, v) = uv(1 + \theta(1 - u)(1 - v)) \quad (12)$$

where $u = F(\lambda_m)$ and $v = F(\lambda_n)$ and the dependence parameter θ in the copula function takes values in [-1, 1], where negative and positive θ indicate negative and positive dependence, respectively, while $\theta = 0$ corresponds to independence between variables.

Therefore, the joint probability density function for variables λ_i and λ_j according to the scalar theorem and FGM copula is expressed as follows:

$$f\left(\lambda_i, \lambda_j\right) = \frac{e^{-\frac{\lambda_i}{\bar{\lambda}_i}-\frac{\lambda_j}{\bar{\lambda}_j}}}{\bar{\lambda}_i \bar{\lambda}_j}\left[1 + \theta\left(1 - 2e^{-\frac{\lambda_i}{\bar{\lambda}_i}}\right)\left(1 - 2e^{-\frac{\lambda_j}{\bar{\lambda}_j}}\right)\right] \quad (13)$$

The marginal probability density functions in (15) are defined as follows:

$$f(\lambda_i) = \frac{1}{\bar{\lambda}_i}e^{-\frac{\lambda_i}{\bar{\lambda}_i}} \quad i = m,n,e \quad \lambda_i > 0 \quad \bar{\lambda}_i = \frac{1}{2\sigma_i^2} \quad (14)$$

2.4. Average secrecy rates of NOMA with optimal power coefficients

The average secrecy rates of downlink NOMA with optimal power coefficients are calculated to assess the system's performance. By optimizing the power coefficients, which determine the power allocation among users, the average secrecy rates can be maximized. This optimization process takes into account the channel conditions, interference, and noise to achieve the highest achievable secrecy rates in NOMA systems. Evaluating the average secrecy rates provides valuable insights into the effectiveness and efficiency of NOMA with optimal power coefficients in ensuring secure and reliable communication.

The average secrecy rates of the downlink NOMA scheme in the optimal power coefficients is expressed as follows:

$$R_{m,ave}^{Sec} \le E_{\lambda_m,\lambda_n,\lambda_e}[\log(1 + \alpha_m^*\lambda_m) - \log(1 + \alpha_m^*\lambda_e)]^+ \quad (15)$$

$$R_{n,ave}^{Sec} \le E_{\lambda_n,\lambda_e}[\log\left(1 + \frac{(1-\alpha_m^*)\lambda_n}{\alpha_m^*\lambda_n + 1}\right) - \log\left(1 + \frac{(1-\alpha_m^*)\lambda_e}{\alpha_m^*\lambda_e + 1}\right)]^+ \quad (16)$$

according to (13), which represents the joint probability density function for two variables, and (15) and (16), the average secrecy rates of the downlink NOMA scheme can be expressed in terms of specific power coefficients, as shown in (17) and (18). These equations provide a mathematical formulation for calculating the average secrecy rates in NOMA systems, taking into account the joint probability density function and the specific power coefficients. By evaluating these expressions, one can analyze and assess the average secure rates achieved in the downlink NOMA scheme.

$$R_{m,ave}^{sec}\left(\alpha_m^* = \frac{1}{\sqrt{1+\lambda_n}+1}\right) \le [\frac{1}{\bar{\lambda}_n}(e^{\left(\frac{1}{\bar{\lambda}_n}+\frac{1}{\bar{\lambda}_e}\right)}\,\mathrm{erf}\left(\sqrt{\frac{1}{\bar{\lambda}_n} - \frac{1}{\bar{\lambda}_e}}\right) -$$
$$e^{\left(\frac{1}{\bar{\lambda}_n}+\frac{1}{\bar{\lambda}_m}\right)}\,\mathrm{erf}\left(\sqrt{\frac{1}{\bar{\lambda}_n} - \frac{1}{\bar{\lambda}_m}}\right)) +$$
$$\frac{\theta}{\bar{\lambda}_n}[e^{\left(\frac{1}{\bar{\lambda}_n}+\frac{1}{\bar{\lambda}_e}\right)}\,\mathrm{erf}\left(\sqrt{\frac{1}{\bar{\lambda}_n} - \frac{1}{\bar{\lambda}_e}}\right) -$$
$$e^{\left(\frac{1}{\bar{\lambda}_n}+\frac{1}{\bar{\lambda}_m}\right)}\,\mathrm{erf}\left(\sqrt{\frac{1}{\lambda_n} - \frac{1}{\bar{\lambda}_m}}\right) +$$
$$e^{\left(\frac{1}{\bar{\lambda}_n}+\frac{1}{2\bar{\lambda}_m}\right)}\,\mathrm{erf}\left(\sqrt{\frac{1}{\bar{\lambda}_n} - \frac{1}{2\bar{\lambda}_m}}\right) -$$

$$e^{\left(\frac{1}{\bar{\lambda}_n}+\frac{1}{2\bar{\lambda}_e}\right)}\,\mathrm{erf}\left(\sqrt{\frac{1}{\bar{\lambda}_n} - \frac{1}{2\bar{\lambda}_e}}\right) +$$
$$2e^{\left(\frac{2}{\bar{\lambda}_n}+\frac{1}{\bar{\lambda}_m}\right)}\,\mathrm{erf}\left(\sqrt{\frac{2}{\bar{\lambda}_n} - \frac{1}{\bar{\lambda}_m}}\right) -$$
$$2e^{\left(\frac{2}{\bar{\lambda}_n}+\frac{1}{\bar{\lambda}_e}\right)}\,\mathrm{erf}\left(\sqrt{\frac{2}{\bar{\lambda}_n} - \frac{1}{\bar{\lambda}_e}}\right) +$$
$$2e^{\left(\frac{2}{\bar{\lambda}_n}+\frac{1}{2\bar{\lambda}_e}\right)}\,\mathrm{erf}\left(\sqrt{\frac{2}{\bar{\lambda}_n} - \frac{1}{2\bar{\lambda}_e}}\right) -$$
$$2e^{\left(\frac{2}{\bar{\lambda}_n}+\frac{1}{2\bar{\lambda}_m}\right)}\,\mathrm{erf}\left(\sqrt{\frac{2}{\bar{\lambda}_n} - \frac{1}{2\bar{\lambda}_m}}\right)]]^+ \quad (17)$$

$$R_{n,ave}^{Sec} \le [\frac{1}{2}e^{\frac{1}{\bar{\lambda}_n}}Ei\left(-\frac{1}{\bar{\lambda}_n}\right) - e^{\frac{1}{\bar{\lambda}_e}}Ei\left(-\frac{1}{\bar{\lambda}_e}\right)]^+ \quad (18)$$

where $[x]^+ \triangleq \max\{0, x\}$.
the proof can be found in **Appendix**.

3. Numerical Resuls

In this section, numerical results regarding average secrecy rates are presented, alongside an examination of the influence of channel correlations on NOMA downlink performance. Both positive and negative dependencies in the channel state are investigated, assuming no prior knowledge of the underlying dependence structure. Through a comparison of performance under independent conditions, it is observed that positive dependence improves performance, whereas negative dependence diminishes the secrecy rate of the stronger user. Additionally, Figure 2 demonstrates that as the gain SNR (Signal-to-Noise Ratio) of each user's channel $(\bar{\lambda}_m, \bar{\lambda}_n)$ increases, the average secrecy rates for a fixed eavesdropping channel SNR $\bar{\lambda}_e$ also increases. This comparison yields insightful observations: positive dependence among the channel states leads to an enhancement in the system's overall performance. This can be attributed to the cooperative effect of correlated fading coefficients, which mitigates interference and bolsters the signal quality. This improvement, in turn, leads to an increase in the secrecy rates, underscoring the beneficial role of positive correlations in the NOMA downlink scheme.
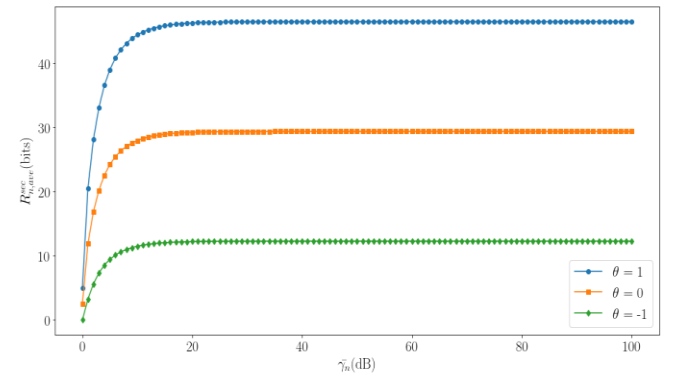

Figure 2. Comparing Average Secrecy Rate of a Stronger User in Downlink Non-Orthogonal Multiple Access (NOMA) Scheme across Different Dependency States
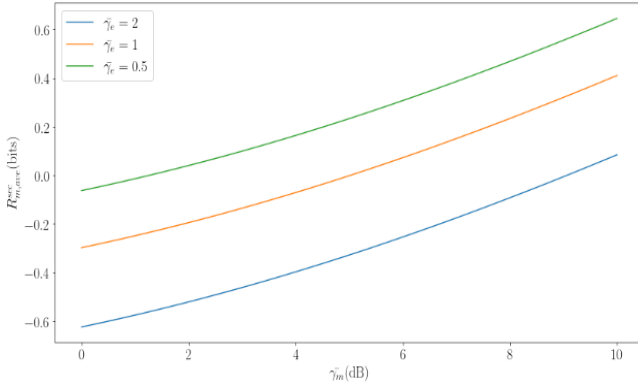
Figure 3. Average Secrecy Rate of the Weaker User in Downlink NOMA and the Impact of Increasing Signal-to-Noise Ratio of the Eavesdropping User on the Secure Rate of the Weaker User

Figure 3 illustrates the average secure rate of the weaker user across various values of $\bar{\lambda}_e$, representing the SNR of the eavesdropper. As observed from the figure, the average secure rate of the weak user exhibits a decreasing trend as the SNR of the eavesdropper increases. Notably, the observed trend showcases that, as anticipated, the average secure rate of the weaker user experiences a declining trajectory as the SNR of the eavesdropper intensifies. This observation resonates with the intuitive notion that a more capable eavesdropper can compromise the security of the transmission, consequently diminishing the achievable secure rates.

On the other hand, the insights gleaned from Figure 3 underscore the paramount importance of securing wireless transmissions against potential eavesdropping threats. As the eavesdropper's capabilities increase, the need for robust security mechanisms becomes more pronounced. Strategies encompassing encryption, authentication, and adaptive power allocation can be invaluable in safeguarding sensitive data against unauthorized access.

Appendix:

$$R_{m,ave}^{Sec} \leq E_{\lambda_m,\lambda_n,\lambda_e}[\log(1+\alpha_m^*\lambda_m) - \log(1+\alpha_m^*\lambda_e)]^+$$
$$= [\mathcal{A} - \mathcal{B}]^+$$

$$\mathcal{A} = \mathcal{A}_1 + \theta(\mathcal{A}_1 - 2\mathcal{A}_2 - 2\mathcal{A}_3 + 4\mathcal{A}_4) \qquad (20)$$

$$\mathcal{B} = \mathcal{B}_1 + \theta(\mathcal{B}_1 - 2\mathcal{B}_2 - 2\mathcal{B}_3 + 4\mathcal{B}_4) \qquad (21)$$

where the following relationship holds:

$$\mathcal{A}_1 = \iint \log\left(1+\frac{\lambda_m}{\sqrt{\lambda_n+1}+1}\right)f(\lambda_m)f(\lambda_n)d\lambda_m d\lambda_n \qquad (22)$$

an equation from a table of integrals [16] is employed in integral calculations.

$$\int_0^\infty e^{-Bx}\ln(1+Ax)\,dx = -\frac{e^{B/A}}{B}Ei\left(-\frac{B}{A}\right) \qquad (23)$$

$$= \int_0^\infty \frac{e^{\frac{\lambda_n}{\bar{\lambda}_n}}}{\bar{\lambda}_n}\left[e^{\frac{\sqrt{\lambda_n+1}+1}{\bar{\lambda}_m}}Ei\left(-\frac{\sqrt{\lambda_n+1}+1}{\bar{\lambda}_m}\right)\right]d\lambda_n \qquad (24)$$

upon applying equation (23) and subsequently simplifying and solving integral (24), the resulting equation is as follows:

$$\mathcal{A}_1 = -\frac{1}{\bar{\lambda}_n}\left(e^{\left(\frac{1}{\bar{\lambda}_n}+\frac{1}{\bar{\lambda}_m}\right)}\operatorname{erf}\left(\sqrt{\frac{1}{\bar{\lambda}_n}-\frac{1}{\bar{\lambda}_m}}\right)\right) \qquad (25)$$

$$\mathcal{A}_2 = \iint \log\left(1+\frac{\lambda_m}{\sqrt{\lambda_n+1}+1}\right)f(\lambda_m)f(\lambda_n)F(\lambda_m)d\lambda_m d\lambda_n$$

$$= \int_0^\infty \frac{e^{\frac{\lambda_n}{\bar{\lambda}_n}}}{\bar{\lambda}_n}\left[e^{\frac{\sqrt{\lambda_n+1}+1}{\bar{\lambda}_m}}Ei\left(-\frac{\sqrt{\lambda_n+1}+1}{\bar{\lambda}_m}\right) - \frac{1}{2}e^{\frac{\sqrt{\lambda_n+1}+1}{\bar{\lambda}_m}}Ei\left(-\frac{\sqrt{\lambda_n+1}+1}{2\bar{\lambda}_m}\right)\right]d\lambda_n \qquad (26)$$

$$\mathcal{A}_2 = -\frac{1}{\bar{\lambda}_n}\left(e^{\left(\frac{1}{\bar{\lambda}_n}+\frac{1}{\bar{\lambda}_m}\right)}\operatorname{erf}\left(\sqrt{\frac{1}{\bar{\lambda}_n}-\frac{1}{\bar{\lambda}_m}}\right)\right) + \frac{1}{2\bar{\lambda}_n}\left(e^{\left(\frac{1}{\bar{\lambda}_n}+\frac{1}{2\bar{\lambda}_m}\right)}\operatorname{erf}\left(\sqrt{\frac{1}{\bar{\lambda}_n}-\frac{1}{2\bar{\lambda}_m}}\right)\right) \qquad (27)$$

$$\mathcal{A}_3 = \iint \log\left(1+\frac{\lambda_m}{\sqrt{\lambda_n+1}+1}\right)f(\lambda_m)f(\lambda_n)F(\lambda_n)d\lambda_m d\lambda_n$$

$$= \int_0^\infty \frac{(e^{\frac{\lambda_n}{\bar{\lambda}_n}}-e^{\frac{2\lambda_n}{\bar{\lambda}_n}})}{\bar{\lambda}_n}\left[\int_0^\infty \log\left(1+\frac{\lambda_m}{\sqrt{\lambda_n+1}+1}\right)\frac{e^{\frac{\lambda_m}{\bar{\lambda}_m}}}{\bar{\lambda}_m}d\lambda_m\right]d\lambda_n$$

$$= \int_0^\infty \frac{(e^{\frac{\lambda_n}{\bar{\lambda}_n}}-e^{\frac{2\lambda_n}{\bar{\lambda}_n}})}{\bar{\lambda}_n}\left[e^{\frac{\sqrt{\lambda_n+1}+1}{\bar{\lambda}_m}}Ei\left(-\frac{\sqrt{\lambda_n+1}+1}{\bar{\lambda}_m}\right) - \frac{1}{2}e^{\frac{\sqrt{\lambda_n+1}+1}{2\bar{\lambda}_m}}Ei\left(-\frac{\sqrt{\lambda_n+1}+1}{2\bar{\lambda}_m}\right)\right]d\lambda_n \qquad (28)$$

$$\mathcal{A}_3 = -\frac{1}{\bar{\lambda}_n}\left(e^{\left(\frac{1}{\bar{\lambda}_n}+\frac{1}{\bar{\lambda}_m}\right)}\operatorname{erf}\left(\sqrt{\frac{1}{\bar{\lambda}_n}-\frac{1}{\bar{\lambda}_m}}\right)\right) + \frac{1}{\bar{\lambda}_n}\left(e^{\left(\frac{2}{\bar{\lambda}_n}+\frac{1}{\bar{\lambda}_m}\right)}\operatorname{erf}\left(\sqrt{\frac{2}{\bar{\lambda}_n}-\frac{1}{\bar{\lambda}_m}}\right)\right) \qquad (29)$$

$$\mathcal{A}_4 = \iint \log\left(1+\frac{\lambda_m}{\sqrt{\lambda_n+1}+1}\right) \times f(\lambda_m)f(\lambda_n)F(\lambda_m)F(\lambda_n)d\lambda_m d\lambda_n \qquad (30)$$

$$= \int_0^\infty \frac{(e^{\frac{\lambda_n}{\bar{\lambda}_n}}-e^{\frac{2\lambda_n}{\bar{\lambda}_n}})}{\bar{\lambda}_n}\left[\int_0^\infty \log\left(1+\frac{\lambda_m}{\sqrt{\lambda_n+1}+1}\right)\frac{(e^{\frac{\lambda_m}{\bar{\lambda}_m}}-e^{\frac{2\lambda_m}{\bar{\lambda}_m}})}{\bar{\lambda}_m}d\lambda_m\right]d\lambda_n \qquad (31)$$

$$= \int_0^\infty \frac{(e^{\frac{\lambda_n}{\bar{\lambda}_n}}-e^{\frac{2\lambda_n}{\bar{\lambda}_n}})}{\bar{\lambda}_n}\left[e^{\frac{\sqrt{\lambda_n+1}+1}{\bar{\lambda}_m}}Ei\left(-\frac{\sqrt{\lambda_n+1}+1}{\bar{\lambda}_m}\right) - \frac{1}{2}e^{\frac{\sqrt{\lambda_n+1}+1}{2\bar{\lambda}_m}}Ei\left(-\frac{\sqrt{\lambda_n+1}+1}{2\bar{\lambda}_m}\right)\right]d\lambda_n$$

$$\mathcal{A}_4 = -\frac{1}{\bar{\lambda}_n}(e^{\left(\frac{1}{\bar{\lambda}_n}+\frac{1}{\bar{\lambda}_m}\right)} \operatorname{erf}\left(\sqrt{\frac{1}{\bar{\lambda}_n}-\frac{1}{\bar{\lambda}_m}}\right) +$$

$$\frac{1}{\bar{\lambda}_n}(e^{\left(\frac{2}{\bar{\lambda}_n}+\frac{1}{\bar{\lambda}_m}\right)} \operatorname{erf}\left(\sqrt{\frac{2}{\bar{\lambda}_n}-\frac{1}{\bar{\lambda}_m}}\right) +$$

$$\frac{1}{2\bar{\lambda}_n}(e^{\left(\frac{1}{\bar{\lambda}_n}+\frac{1}{2\bar{\lambda}_m}\right)} \operatorname{erf}\left(\sqrt{\frac{1}{\bar{\lambda}_n}-\frac{1}{2\bar{\lambda}_m}}\right) -$$

$$\frac{1}{2\bar{\lambda}_n}(e^{\left(\frac{2}{\bar{\lambda}_n}+\frac{1}{2\bar{\lambda}_m}\right)} \operatorname{erf}\left(\sqrt{\frac{2}{\bar{\lambda}_n}-\frac{1}{2\bar{\lambda}_m}}\right)$$

$$(32)$$

for the computation of the value of $\mathcal{A}$, the combination and simplification of equations (25), (27), (29), and (32) can be performed. By performing the necessary mathematical operations and substitutions, the value of $\mathcal{A}$ can be determined.

Likewise, for the calculation of $\mathcal{B}_i$, the particular method or formula detailed in the provided methodology would be required.

$$\mathcal{B}_1 = \iint \log\left(1+\frac{\lambda_e}{\sqrt{\lambda_n+1}+1}\right)f(\lambda_e)f(\lambda_n)d\lambda_e d\lambda_n$$

$$= \int_0^\infty \frac{e^{\frac{\lambda_n}{\bar{\lambda}_n}}}{\bar{\lambda}_n}\left[e^{\frac{\sqrt{\lambda_n+1}+1}{\bar{\lambda}_e}}Ei\left(-\frac{\sqrt{\lambda_n+1}+1}{\bar{\lambda}_e}\right)\right]d\lambda_n$$

$$(33)$$

$$\mathcal{B}_1 = -\frac{1}{\bar{\lambda}_n}(e^{\left(\frac{1}{\bar{\lambda}_n}+\frac{1}{\bar{\lambda}_e}\right)} \operatorname{erf}\left(\sqrt{\frac{1}{\bar{\lambda}_n}-\frac{1}{\bar{\lambda}_e}}\right) \qquad (34)$$

$$\mathcal{B}_2 = \iint \log\left(1+\frac{\lambda_e}{\sqrt{\lambda_n+1}+1}\right)f(\lambda_e)f(\lambda_n)F(\lambda_e)d\lambda_e d\lambda_n$$

$$= \int_0^\infty \frac{e^{\frac{\lambda_n}{\bar{\lambda}_n}}}{\bar{\lambda}_n}\left[e^{\frac{\sqrt{\lambda_n+1}+1}{\bar{\lambda}_e}}Ei\left(-\frac{\sqrt{\lambda_n+1}+1}{\bar{\lambda}_e}\right) - \right.$$

$$\left. \frac{1}{2}e^{\frac{\sqrt{\lambda_n+1}+1}{2\bar{\lambda}_e}}Ei\left(-\frac{\sqrt{\lambda_n+1}+1}{2\bar{\lambda}_e}\right)\right]d\lambda_n$$

$$(35)$$

$$\mathcal{B}_2 = -\frac{1}{\bar{\lambda}_n}(e^{\left(\frac{1}{\bar{\lambda}_n}+\frac{1}{\bar{\lambda}_e}\right)} \operatorname{erf}\left(\sqrt{\frac{1}{\bar{\lambda}_n}-\frac{1}{\bar{\lambda}_e}}\right) +$$

$$\frac{1}{2\bar{\lambda}_n}(e^{\left(\frac{1}{\bar{\lambda}_n}+\frac{1}{2\bar{\lambda}_e}\right)} \operatorname{erf}\left(\sqrt{\frac{1}{\bar{\lambda}_n}-\frac{1}{2\bar{\lambda}_e}}\right)$$

$$(36)$$

$$\mathcal{B}_3 = \iint \log\left(1+\frac{\lambda_e}{\sqrt{\lambda_n+1}+1}\right)f(\lambda_e)f(\lambda_n)F(\lambda_n)d\lambda_e d\lambda_n$$

$$= \int_0^\infty \frac{(e^{\frac{\lambda_n}{\bar{\lambda}_n}-e^{\frac{2\lambda_n}{\bar{\lambda}_n}}})}{\bar{\lambda}_n}\left[\int_0^\infty \log\left(1+\frac{\lambda_e}{\sqrt{\lambda_n+1}+1}\right)\frac{e^{\frac{\lambda_e}{\bar{\lambda}_e}}}{\bar{\lambda}_e}d\lambda_e\right]d\lambda_n$$

$$= \int_0^\infty \frac{(e^{\frac{\lambda_n}{\bar{\lambda}_n}} - e^{\frac{2\lambda_n}{\bar{\lambda}_n}})}{\bar{\lambda}_n}\left[e^{\frac{\sqrt{\lambda_n+1}+1}{\bar{\lambda}_e}}Ei\left(-\frac{\sqrt{\lambda_n+1}+1}{\bar{\lambda}_e}\right) - \right.$$

$$\left. \frac{1}{2}e^{\frac{\sqrt{\lambda_n+1}+1}{2\bar{\lambda}_e}}Ei\left(-\frac{\sqrt{\lambda_n+1}+1}{2\bar{\lambda}_e}\right)\right]d\lambda_n$$

$$(37)$$

$$\mathcal{B}_3 =$$
$$-\frac{1}{\bar{\lambda}_n}(e^{\left(\frac{1}{\bar{\lambda}_n}+\frac{1}{\bar{\lambda}_e}\right)} \operatorname{erf}\left(\sqrt{\frac{1}{\bar{\lambda}_n}-\frac{1}{\bar{\lambda}_e}}\right) + \frac{1}{\bar{\lambda}_n}(e^{\left(\frac{2}{\bar{\lambda}_n}+\frac{1}{\bar{\lambda}_e}\right)} \operatorname{erf}\left(\sqrt{\frac{2}{\bar{\lambda}_n}-\frac{1}{\bar{\lambda}_e}}\right)$$

$$(38)$$

$$\mathcal{B}_4 = \iint \log\left(1+\frac{\lambda_e}{\sqrt{\lambda_n+1}+1}\right)f(\lambda_e)f(\lambda_n)F(\lambda_e)F(\lambda_n)d\lambda_e d\lambda_n$$

$$(39)$$

$$= \int_0^\infty \frac{(e^{\frac{\lambda_n}{\bar{\lambda}_n}-e^{\frac{2\lambda_n}{\bar{\lambda}_n}}})}{\bar{\lambda}_n}\left[\int_0^\infty \log\left(1+\frac{\lambda_e}{\sqrt{\lambda_n+1}+1}\right)\frac{(e^{\frac{\lambda_e}{\bar{\lambda}_e}-e^{\frac{2\lambda_e}{\bar{\lambda}_e}}})}{\bar{\lambda}_e}d\lambda_e\right]d\lambda_n$$

$$= \int_0^\infty \frac{(e^{\frac{\lambda_n}{\bar{\lambda}_n}} - e^{\frac{2\lambda_n}{\bar{\lambda}_n}})}{\bar{\lambda}_n}\left[e^{\frac{\sqrt{\lambda_n+1}+1}{\bar{\lambda}_e}}Ei\left(-\frac{\sqrt{\lambda_n+1}+1}{\bar{\lambda}_e}\right) - \right]$$

$$\frac{1}{2}e^{\frac{\sqrt{\lambda_n+1}+1}{2\bar{\lambda}_e}}Ei\left(-\frac{\sqrt{\lambda_n+1}+1}{2\bar{\lambda}_e}\right)\right]d\lambda_n$$

$$(40)$$

$$\mathcal{B}_4 = -\frac{1}{\bar{\lambda}_n}(e^{\left(\frac{1}{\bar{\lambda}_n}+\frac{1}{\bar{\lambda}_e}\right)} \operatorname{erf}\left(\sqrt{\frac{1}{\bar{\lambda}_n}-\frac{1}{\bar{\lambda}_e}}\right) +$$

$$\frac{1}{\bar{\lambda}_n}(e^{\left(\frac{2}{\bar{\lambda}_n}+\frac{1}{\bar{\lambda}_e}\right)} \operatorname{erf}\left(\sqrt{\frac{2}{\bar{\lambda}_n}-\frac{1}{\bar{\lambda}_e}}\right) +$$

$$\frac{1}{2\bar{\lambda}_n}(e^{\left(\frac{1}{\bar{\lambda}_n}+\frac{1}{2\bar{\lambda}_e}\right)} \operatorname{erf}\left(\sqrt{\frac{1}{\bar{\lambda}_n}-\frac{1}{2\bar{\lambda}_e}}\right) -$$

$$\frac{1}{2\bar{\lambda}_n}(e^{\left(\frac{2}{\bar{\lambda}_n}+\frac{1}{2\bar{\lambda}_e}\right)} \operatorname{erf}\left(\sqrt{\frac{2}{\bar{\lambda}_n}-\frac{1}{2\bar{\lambda}_e}}\right)$$

$$(41)$$

4. Conclusion

In this paper, a thorough comparison was made between NOMA and OMA schemes. Analysis of performance measures showed that NOMA with certain optimal power coefficients outperforms OMA in terms of average secrecy rates. Through the utilization of copula functions to model the correlation among channel coefficients, the inherent dependences among the fading coefficients were determined. Considering these dependencies and employing the computed specific optimal power coefficients, a substantial enhancement in the average NOMA secrecy rates is exhibited when compared to independent NOMA scenarios. These findings highlight the importance of combining channel dependencies and optimizing power factors in achieving improved performance in NOMA-based wireless communication systems.

5. References

[1] Wang, Bichai, et al. "Comparison study of non-orthogonal multiple access schemes for 5G." *2015 IEEE International Symposium on Broadband Multimedia Systems and Broadcasting*. IEEE, 2015.

[2] Wu, Z., Lu, K., Jiang, C., and Shao, X., "Comprehensive Study and Comparison on 5G NOMA Schemes," in *IEEE Access*, Vol. 6, pp. 18511-18519, 2018.

[3] Chen, Z., Ding, Z., Dai, X., and Zhang, R., "An Optimization Perspective of the Superiority of NOMA Compared to Conventional OMA," in *IEEE Transactions on Signal Processing*, Vol. 65, No. 19, pp. 5191-5202, 1 Oct.1, 2017.

[4] Liu, Y., Pan, G., Zhang, H., and Song, M., "On the Capacity Comparison Between MIMO-NOMA and MIMO-OMA," in *IEEE Access*, Vol. 4, pp. 2123-2129, 2016.

[5] El-Sayed, Mohamed, M., Ahmed, S., Ibrahim, and Mohamed M., Khairy. "Power allocation strategies for non-orthogonal multiple access." *2016 international conference on selected topics in mobile & wireless networking (MoWNeT)*. IEEE, 2016.

[6] Khan, W. U., Jameel, F., Jamshed, M. A., Pervaiz, H., Khan, S., Liu, J., "Efficient power allocation for noma-enabled iot networks in 6g era", Phys. Commun., 39, pp. 101043, 2020.

[7] Wu, Y., Khisti, A., Xiao, C., Caire, G., Wong, K. -K., and Gao, X., "A Survey of Physical Layer Security Techniques for 5G Wireless Networks and Challenges Ahead," in *IEEE Journal on Selected Areas in Communications*, Vol. 36, No. 4, pp. 679-695, April 2018.

[8] Zhang, Y., Wang, H. -M., Yang, Q., and Ding, Z., "Secrecy Sum Rate Maximization in Non-orthogonal Multiple Access", in *IEEE Communications Letters*, Vol. 20, No. 5, pp. 930-933, May 2016.

[9] Zhang, Y., Wang, H. -M., Yang, Q., and Ding, Z., "Secrecy Sum Rate Maximization in Non-orthogonal Multiple Access", in *IEEE Communications Letters*, Vol. 20, No. 5, pp. 930-933, May 2016.

[10] Cao, K., *et al.*, "Achieving Reliable and Secure Communications in Wireless-Powered NOMA Systems", in *IEEE Transactions on Vehicular Technology*, Vol. 70, No. 2, pp. 1978-1983, Feb. 2021.

[11] Zhang, C., Jia, F., Zhang, Z., Ge, J., and Gong, F., "Physical Layer Security Designs for 5G NOMA Systems with a Stronger Near-End Internal Eavesdropper", in *IEEE Transactions on Vehicular Technology*, Vol. 69, No. 11, pp. 13005-13017, Nov. 2020.

[12] Ghadi, F. R., and Hodtani, G. A., "Copula-Based Analysis of Physical Layer Security Performances Over Correlated Rayleigh Fading Channels", in *IEEE Transactions on Information Forensics and Security*, Vol. 16, pp. 431-440, 2021.

[13] Nelson, R. B., 'An introduction to copulas' (Springer Science & Business Media, New York, NY, 2007.

[14] Shemyakin A., Kniazev A., "Introduction to Bayesian estimation and copula models of dependence", John Wiley & Sons., 2017.

[15] Hamamreh, J. M., Furqan, H. M., and Arslan, H., "Classifications and applications of physical layer security techniques for confidentiality: A comprehensive survey", *IEEE Commun. Surveys Tuts.*, pp. 1–1, 2018.

[16] Geller, M., Ng, E. W., "A table of integrals of the exponential integral", *J. Res. Natl. Bur. Stand*, Vol. 71, pp. 1-20, 1969.